Spectroscopy and Absolute Reactivity of Ketenes in Acetonitrile Studied by Laser Flash Photolysis with Time-Resolved Infrared Detection

Brian D. Wagner,*,†,‡ Bradley R. Arnold,† Gerald S. Brown,† and Janusz Lusztyk*,†

Contribution from the Steacie Institute for Molecular Sciences, National Research Council of Canada, Ottawa, Ontario, Canada K1A 0R6, and the Department of Chemistry, University of Prince Edward Island, Charlottetown, Prince Edward Island, Canada C1A 4P3

Received December 2, 1996

Abstract: Laser flash photolysis with time-resolved infrared detection of transients (LFP-TRIR) has been used to study the IR spectroscopy and reactivity of a number of substituted ketenes, prepared by the 308-nm photolysis of α-diazocarbonyl precursors in acetonitrile solution at room temperature. The correlation of the experimental ketene asymmetric stretching frequency to the Swain−Lupton field (*F*) and resonance (*R*) effect substituent parameters was unsatisfactory, whereas the correlation to the inductive substituent parameter (σ_I) of Charton gave excellent results. This suggests that the asymmetric stretching frequency of substituted ketenes depends mainly on the inductive (*i.e.*, field) effect of the substituents. The mechanism and kinetics of the reactions of these ketenes with various amines in acetonitrile were also studied. An intermediate species identified as either zwitterionic ylide or amide enol formed in the nucleophilic addition of the secondary amine to the C_α of the ketene is observed by TRIR. The decay of this species is assisted by the amine and is concomitant with the formation of an amide, the final product of the reaction. Our kinetic data on ketene amine reactions show a general trend, indicating a much higher reactivity (*ca.* 3 orders of magnitude difference in the corresponding rate constants) of secondary amines compared with that of tertiary amines. Secondary diethylamine shows reactivity similar to those observed for primary amines, while secondary piperidine seems to be, in general, somewhat more reactive. The observed trend is rationalized in terms of the steric effects exerted by both amine and ketene substituents. Our data on para-substituted phenyl ketenes provide support for the negative charge development on the ketene moiety in the transition state, with electron-withdrawing substituents accelerating and electron-releasing substituents slowing down the addition reaction.

Introduction

Ketenes are extremely important reactive species, which occur as transients in numerous thermal and photochemical reactions.[1−5] In many cases, ketenes have relatively weak UV absorption bands below 400 nm, making them difficult to resolve from other species in UV laser flash photolysis (LFP), although a number of studies of ketene reactivity employing this technique have been reported.[6−10] However, all ketenes exhibit a very strong and characteristic IR band in the region of 2100 cm^{-1}, arising from the out-of-phase or antisymmetric stretch of the C═C═O moiety.[11] The IR spectroscopy of ketenes has been extensively studied in cryogenic matrices[12−14] and has been applied recently to investigate ketene reactions toward nucleophiles in this medium.[15,16] We[17−21] and others[22] have also recently demonstrated that LFP with time-resolved infrared

† National Research Council of Canada. NRCC publication 40855.
‡ University of Prince Edward Island.

(1) (a) Patai, S., Ed. *The Chemistry of Ketenes, Allenes, and Related Compounds*; John Wiley and Sons: New York, 1980. (b) Tidwell, T. T. *Ketenes*; John Wiley and Sons: New York, 1995.
(2) Seikaty, H. R.; Tidwell, T. T. *Tetrahedron* **1986**, *42*, 2587−2613.
(3) Tidwell, T. T. *Acc. Chem. Res* **1990**, *23*, 273−279.
(4) Snider, B. B. *Chem. Rev.* **1988**, *88*, 793−811.
(5) Ye, T.; McKervey, M. A. *Chem. Rev.* **1994**, *94*, 1091−1160.
(6) Allen, A. D.; Kresge, A. J.; Schepp, N. P.; Tidwell, T. T. *Can. J. Chem.* **1987**, *65*, 1719−1723.
(7) Andraos, J.; Kresge, A. J. *J. Am. Chem. Soc.* **1992**, *114*, 5643−5646.
(8) Andraos, J.; Chiang, Y.; Huang, C.-G.; Kresge, A. J.; Scaiano, J. C. *J. Am. Chem. Soc.* **1993**, *115*, 10605−10610.
(9) Andraos, J.; Kresge, A. J. *J. Photochem. Photobiol. A* **1991**, *57*, 165−173.
(10) Allen, A. D.; Andraos, J.; Kresge, A. J.; McAllister, M. A.; Tidwell, T. T. *J. Am. Chem. Soc.* **1992**, *114*, 1878−1879.
(11) Lin-Vien, D.; Cothup, N. B.; Fatetey, W. G.; Graselli, J. G. *The Handbook of Infrared and Raman Characteristic Frequencies of Organic Molecules*; Academic: San Diego, CA, 1991.
(12) Moore, C. B.; Pimentel, G. C. *J. Chem. Phys.* **1963**, *38*, 2816−2829.
(13) Torres, M.; Ribo, J.; Clement, A.; Strausz, O. P. *Nouv. J. Chim.* **1981**, *5*, 351−352.
(14) Maier, G.; Preiss, T.; Reisenauer, H. P.; Hess, B. A., Jr.; Schaad, L. J. *J. Am. Chem. Soc.* **1994**, *116*, 2014−2018.
(15) Qiao, G. G.; Andraos, J.; Wentrup, C. *J. Am. Chem. Soc.* **1996**, *118*, 5634−5638.
(16) Visser, P.; Zuhse, R.; Wong, M. W.; Wentrup, C. *J. Am. Chem. Soc.* **1996**, *118*, 12598−12602.
(17) Arnold, B. R.; Brown, C. E.; Lusztyk, J. *J. Am. Chem. Soc.* **1993**, *115*, 1576−1577.
(18) Wagner, B. D.; Zgierski, M. Z.; Lusztyk, J. *J. Am. Chem. Soc.* **1994**, *116*, 6433−6434.
(19) Allen, A. D.; Colomvakos, J. D.; Egle, I.; Lusztyk, J.; McAllister, M. A.; Tidwell, T. T.; Wagner, B. D.; Zhao, D. *J. Am. Chem. Soc.* **1995**, *117*, 7552−7553.
(20) Camara de Lucas, N.; Netto-Ferreira, J. C.; Andraos, J.; Lusztyk, J.; Wagner, B. D.; Scaiano, J. C. *Tetrahedron Lett.* **1997**, *38*, 5147−5150.
(21) Allen, A. D.; Colomvakos, J. D.; Diederich, F.: Egle, I.; Hao, X.; Liu, R.; Lusztyk, J.; Ma, J.; McAllister, M. A.; Rubin, Y.; Sung, K.; Tidwell, T. T.; Wagner, B. D. *J. Am. Chem. Soc.* **1997**, *119*, 12125−12130.
(22) Oishi, S.; Watanabe, Y.; Kuriyama, Y. *Chem. Lett.* **1994**, 2187−2190.

S0002-7863(96)04155-8 CCC: $15.00
Published on Web 02/14/1998

detection (LFP-TRIR) is ideally suited for both mechanistic and kinetic studies of ketenes in solution since the characteristic spectroscopic region near 2100 cm^{-1} is transparent to most solvents and void of absorptions due to other photogenerated transients and products. In this paper, we employ LFP-TRIR for systematic studies of the infrared spectroscopic properties of ketenes and explore the mechanism and kinetics of the ketene amine reactions.

Ketene stretching frequencies are very sensitive to substitution, with values of the asymmetric stretch reported from 2085 to 2197 cm^{-1}.[11] There have been a number of efforts to correlate these observed frequencies to substituent parameters. Gano and Jacob[23] used experimental frequencies obtained from the literature for a set of symmetrically disubstituted ketenes to test the correlation to the field or inductive (F) and resonance (R) parameters model of Swain and Lupton.[24,25] These parameters were chosen because of their generality and the useful separation of the substituent effect into field and resonance components. In this approach, the ketene stretching frequencies were fit to a model equation containing F and R as two independent parameters. A good correlation with the following fit parameters was obtained:

$$\bar{\nu}_x\,(\mathrm{cm}^{-1}) = 2124 + 24F_x + 30R_x \qquad (1)$$

However, this correlation was based on a rather limited data set of five experimental frequencies, which were measured in different media (gas phase, cryogenic matrix). McAllister and Tidwell[26] extended this approach by using ketene stretching frequencies obtained by *ab initio* calculations for both symmetrically disubstituted and monosubstituted ketenes. Their calculated frequencies agreed within *ca.* 10 cm^{-1} with the available experimental values but had a poorer correlation (r = 0.87) than Jacob and Gano's, with a near zero contribution from the resonance effect:

$$\bar{\nu}_x\,(\mathrm{cm}^{-1}) = 2124 + 91F_x - 6R_x \qquad (2)$$

They obtained a similar correlation (r = 0.86) by fitting their data just to the field parameter F. Obviously, there is a need for a larger set of experimental ketene frequencies obtained under standardized experimental conditions to allow for more definitive delineation of the field and resonance effects.[27]

Nucleophilic addition reactions of ketenes are well-known and have been extensively reviewed.[1−5] The vast majority of studies, however, have dealt with the hydration kinetics of ketenes in aqueous or mixed aqueous/organic solvent.[6,8−10,28,29] It has been shown that the acid-catalyzed reaction involves rate-limiting proton transfer to C_β perpendicular to the plane of the ketene, whereas reaction with OH^- or H_2O involves nucleophilic attack on C_α in the plane of the ketene.[6] Andraos and Kresge have reported kinetic studies of the reaction of diphenyl ketene with various bases in aqueous solution.[7] They concluded from the observed reactivities that the reaction proceeds via direct nucleophilic attack of the base on the carbonyl carbon of the ketene (C_α) and not via base-catalyzed hydration.

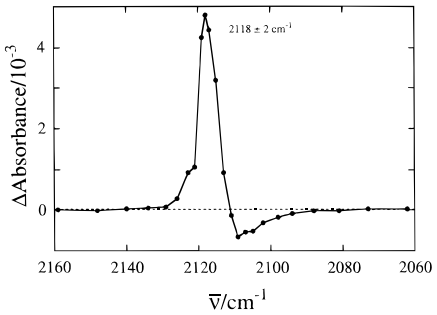

Figure 1. TRIR spectrum of phenyl ketene observed 4 μs after 308-nm photolysis of α-diazoacetophenone in N_2-saturated CH_3CN solution.

Scheme 1

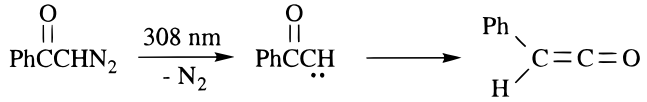

There have been relatively few reported studies of ketene reactivities in nonaqueous media. Satchell and co-workers[30−33] studied the reactions of ketene, dimethyl ketene, and diphenyl ketene with anilines in ether and benzene. They reported the rate law

$$\mathrm{rate} = (k_1[\mathrm{ArNH_2}] + k_2[\mathrm{ArNH_2}]^2)[\mathrm{ketene}] \qquad (3)$$

for which they proposed the existence of two different transition states, one involving one aniline molecule, the other involving two. These workers also studied the addition of bulky alcohols to ketene in isooctane and CCl_4 solutions and again reported nonlinear quenching plots.[34] In this case, the nonlinearity was explained by a mechanism involving the more reactive (relative to the monomer) trimers at high alcohol concentrations.

Results and Discussion

Substituent Effects on the Ketene Asymmetric Stretching Frequency. In this paper, we report the results on the IR spectroscopy of a number of ketenes, studied by LFP-TRIR in acetonitrile at room temperature. All except for one of the ketenes were generated by the 308-nm photolysis of the corresponding α-diazocarbonyl compounds, via the Wolff rearrangement of the initial carbene.[35−37] For example, phenyl ketene was generated via photolysis of α-diazoacetophenone, as illustrated in Scheme 1. Ketene VIIIa was generated from the 308-nm photolysis of 2*H*-pyran-2-one.[17] In all cases, extremely strong and well-defined absorptions were observed

(23) Gano, J. E.; Jacob, E. J. *Spectrochim. Acta* **1987**, *43A*, 1023−1025.
(24) Swain, C. G.; Lupton, E. C., Jr. *J. Am. Chem. Soc.* **1968**, *90*, 4328−4337.
(25) Swain, C. G.; Unger, S. H.; Rosenquist, N. R.; Swain, M. S. *J. Am. Chem. Soc.* **1983**, *105*, 492−502.
(26) McAllister, M. A.; Tidwell, T. T. *Can. J. Chem.* **1994**, *72*, 882−887.
(27) The only previous experimental results that we are aware of on the substituent effect on the ketene stretching frequencies in solution are that by: Melzer, A.; Jenny, E. F. *Tetrahedron Lett.* **1968**, 4503−4506. The values in 1,2-dichloroethane for the relevant diphenyl ketene, 4,4′-dimethoxydiphenyl ketene, and 4,4′-dinitrodiphenyl ketene are 2100, 2096, and 2109 cm^{-1}, respectively.
(28) Allen, A. D.; Tidwell, T. T. *J. Am. Chem. Soc.* **1987**, *109*, 2774−2780.
(29) Allen, A. D.; Stevenson, A.; Tidwell, T. T. *J. Org. Chem.* **1989**, *54*, 2843−2848.
(30) Briody, J. M.; Satchell, D. P. N. *Tetrahedron* **1966**, *22*, 2649−2653.
(31) Lillford, P. J.; Satchell, D. P. N. *J. Chem. Soc. B* **1967**, 360−365.
(32) Lillford, P. J.; Satchell, D. P. N. *J. Chem. Soc. B* **1968**, 54−57.
(33) Lillford, P. J.; Satchell, D. P. N. *J. Chem. Soc. B* **1970**, 1016−1019.
(34) Donohoe, G.; Satchell, D. P. N.; Satchell, R. S. *J. Chem. Soc., Perkins Trans. 2* **1990**, 1671−1674.
(35) Meier, H.; Zeller, K.-P. *Angew. Chem., Int. Ed. Engl.* **1975**, *14*, 32−43.
(36) Tomioka, H.; Okuno, H.; Izawa, Y. *J. Org. Chem.* **1980**, *45*, 5278−5283.
(37) Scott, A. P.; Nobes, R. H.; Schaefer, H. F., III; Radom, L. *J. Am. Chem. Soc.* **1994**, *116*, 10159−10164.

Table 1. Observed Ketene Stretching Frequencies in Acetonitrile at 23 °C[a]

precursors						$\bar{R}_2$ substituent parameters		
no.	structure	no.	R_1	R_2	$\bar{\nu}$/cm^{-1}	*F*	*R*	σ_I
I	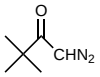	Ia	H	*t*-Bu	2108	−0.02	−0.18	−0.01
II	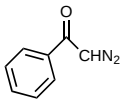	IIa	H	Ph	2118	0.12	−0.13	0.12
III	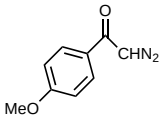	IIIa	H	*p*-MeOPh	2115	0.13	−0.21	0.11
IV	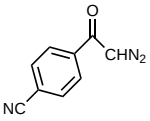	IVa	H	*p*-CNPh	2120			
V	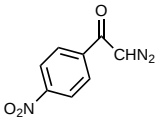	Va	H	*p*-NO_2Ph	2122	0.26	0.0	0.22
VI	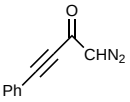	VIa	H	PhC≡C	2130	0.15	0.01	0.33
VII	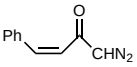	VIIa	H	PhCH═CH	2116	0.10	−0.17	
VIII		VIIIa	H		2127	0.29	−0.16	
IX		IXa	Ph	Ph	2100			
X	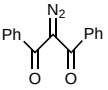	Xa	Ph		2119			

[a] All frequencies are ± 2 cm^{-1}. The substituent parameters F, R, and σ_I are given for monosubstituted ketenes where available.

in the ketene stretching region. The TRIR spectrum of phenyl ketene in acetonitrile is shown in Figure 1. A strong, sharp band is observed with a maximum at 2118 ± 2 cm^{-1}, as well as a weak bleaching at 2107 cm^{-1} resulting from the depletion of the diazo band of the α-diazoacetophenone precursor. Similar spectra were obtained for the other ketenes studied; the observed ketene stretching frequencies are given in Table 1. The observed frequencies for the monosubstituted ketenes range from 2108 to 2130 cm^{-1}, a total range of only 22 cm^{-1}. However, since the data were obtained under standardized experimental conditions, the set of seven monosubstituted ketenes does provide a useful data set for correlations to substituent parameters. Table 1 also includes the values of *F* and *R* for these substituents, taken from ref 38. The fit of the experimental frequencies to *F* and *R* yielded the following equation:

$$\bar{\nu}_x\,(\mathrm{cm}^{-1}) = 2117 + 43F_x + 35R_x \qquad (4)$$

This is in reasonable agreement with the data obtained by Gano and Jacob[23] (eq 1), with nearly equal contributions from the field and resonance terms. However, our correlation coefficient was much poorer, $r = 0.858$ (Figure 2). The fit is especially bad in the case of *p*-nitrophenyl ketene. The correlation of the observed frequencies to just the field parameter *F* was even poorer ($r = 0.768$).

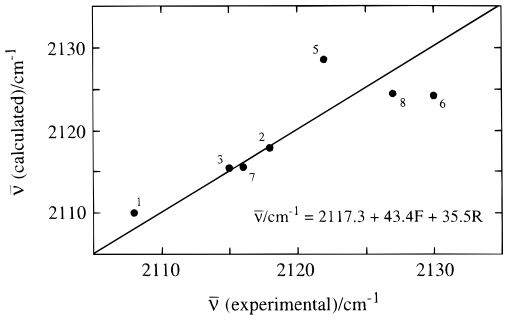

Figure 2. Plot of ketene stretching frequencies calculated from eq 4 *vs* experimental frequencies.

There has been some criticism of the Swain−Lupton approach.[39,40] Hoefnagel *et al.*[39] applied the Swain−Lupton equation to a number of experimental systems, including the pK_a of substituted phenols and anilinium ions. Gross deviations

(38) Hansch, C.; Leo, A.; Taft, R. W. *Chem. Rev.* **1991**, *91*, 165−195.

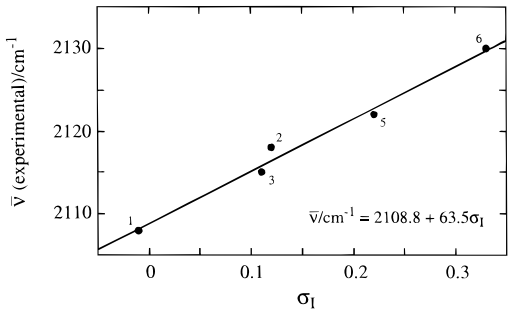

Figure 3. Plot of experimental ketene stretching frequencies *vs* Charton's substituent parameter σ_I.

from the experimental values were observed, leading to the conclusion that the Swain−Lupton approach is much more limited than was originally claimed. Charton[40] came to the same conclusion and proposed an alternative parameter, σ_I. This is purely an inductive effect parameter, with no contribution from delocalization (resonance) effects. Charton showed that for a number of systems which are free from resonance effects, σ_I was a much better representation of the localized field effect than was *F*. Unfortunately, the values for this parameter were only available for five of the monosubstituted ketenes that we studied.[40] An excellent correlation ($r = 0.993$) was obtained for this admittedly limited data set, as shown in Figure 3. The fit equation obtained was

$$\bar{\nu}\,(\mathrm{cm}^{-1}) = 2108.8 + 63.5\sigma_I \qquad (5)$$

The excellent correlation observed with σ_I may suggest that only the inductive, or localized field, effect of substituents is important in determining the stretching frequency of the monosubstituted ketenes. This is in agreement with the conclusions of McAllister and Tidwell;[26] however, we find that σ_I is a much better measure of the inductive effect than is *F*. Equation 5 should provide a good predictive tool for the expected frequency of the monosubstituted ketenes; obviously more experimental frequencies would be useful for further testing the validity of this equation.

The observed correlation of the ketene stretching frequency with the inductive substituent effect parameter can be explained in terms of the following two major resonance forms for monosubstituted ketenes:

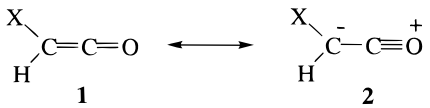

1 **2**

The presence of electron-accepting groups (large σ_I) will tend to stabilize the carbanion in resonance form **2**, increasing its contribution to the overall structure. This increases the CO bond order and, hence, increases the observed CO stretching frequency. In the case of electron releasing groups (small or negative σ_I), the carbanion form **2** is destabilized, and thus, the CO bond order is reduced, and the CO stretching frequency is lowered.

Efforts were made to expand the observed range of ketene frequencies. Our attempts to observe ketenes with heteroatom substituents (expected to have larger shifts in the stretching frequency) from the corresponding α-diazocarbonyl precursors in LFP-TRIR experiments were unsuccessful. For example, we failed to observe the expected[36] ethoxy ketene upon photolysis of the commercially available ethyl diazoacetate. Similarly, photolysis of *N*,*N*-dimethyldiazoacetamide (synthesized in our lab) did not produce detectable amounts of the expected *N*,*N*-dimethylamino ketene. Rando[41] and Tomioka *et al.*[42] reported predominant formation of the cyclic lactam products (formed by intramolecular C−H insertion of the initially formed carbene) upon photolysis of this compound, indicating that the yield of the ketene product is relatively low.

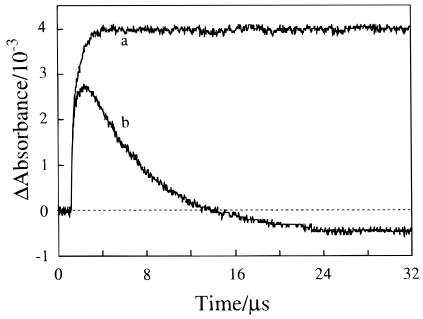

Figure 4. Observed phenyl ketene kinetic traces measured at 2118 cm^{-1} in the absence of quencher (a) and in the presence of 0.3 mM diethylamine (b). The fit of the latter trace to a single-exponential decay gave an excellent fit with a first-order decay constant (k_{obs}) of 1.6 × 10^5 s^{-1}.

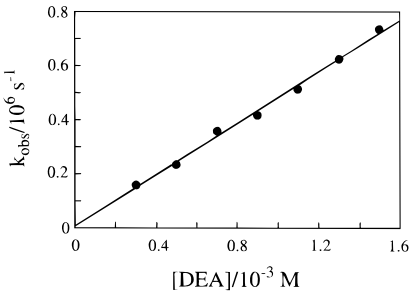

Figure 5. Quenching plot of the observed first-order decay constant (k_{obs}) for the decay of phenyl ketene *vs* the concentration of diethylamine in CH_3CN. Linear least-squares analysis yields a slope of 4.8 × 10^8 M^{-1} s^{-1} with a correlation coefficient of 0.994.

Nucleophilic Addition Reactions of Amines with Ketenes. Kinetic studies of the reactions of a family of ketenes with a wide variety of amines are reported herein. In the absence of added quencher, all the ketenes studied except VIIIa were stable on the longest available experimental time scale (128 μs), indicating lifetimes of greater than 500 μs. However, the lifetimes of all the ketenes studied were shortened by added amines. Figure 4 shows the observed kinetic trace of phenyl ketene in the absence of quencher (a) and in the presence of 0.3 mM diethylamine (b). A stable signal is observed in the former case, while in the latter, a well-defined first-order decay is recorded. Assuming pseudo-first-order kinetics, the observed rate constant of ketene decay (k_{obs}) as a function of added quencher concentration ([Q]) is given by

$$k_{obs} = k_o + k_q[Q] \qquad (6)$$

where k_o is the observed decay rate constant in the absence of quencher and k_q is the second-order quenching rate constant. The values of k_q were thus obtained from the slopes of the plots of k_{obs} *vs* [Q]. Figure 5 shows a representative quenching plot for the case of phenyl ketene reacting with diethylamine. Within

(39) Hoefnagel, A. J.; Oosterbeek, W.; Wepster, B. M. *J. Org. Chem.* **1984**, *49*, 1993−1997.
(40) Charton, M. *J. Org. Chem.* **1984**, *49*, 1997−2001.
(41) Rando, R. R. *J. Am. Chem. Soc.* **1970**, *92*, 6706−6707.
(42) Tomioka, H.; Kitagawa, H.; Izawa, Y. *J. Org. Chem.* **1979**, *44*, 3072−3075.

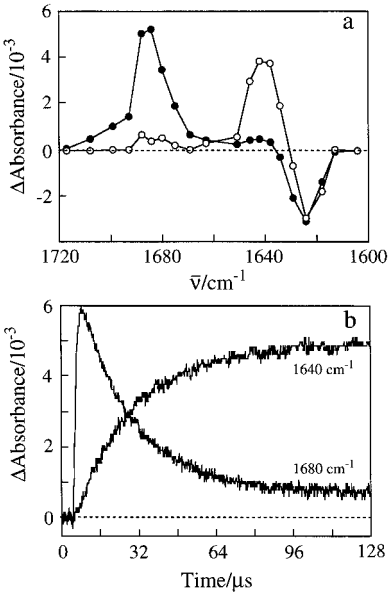

Figure 6. (a) TRIR spectrum in the carbonyl region observed 2 μs (●) and 60 μs (○) after 308-nm photolysis of α-diazoacetophenone in the presence of 2.5 mM diethylamine in N_2-saturated CH_3CN solution. (b) Observed kinetic traces at 1680 and 1640 cm^{-1}.

the explored concentration range of the quencher, good linearity of the plot is obtained, yielding a rate constant of 4.8×10^8 M^{-1} s^{-1}.

Upon photolysis of α-diazoacetophenone in the presence of diethylamine, a transient species with a band maximum at 1680 cm^{-1} was observed to grow in with kinetics identical with that observed for the decay of the phenyl ketene band at 2116 cm^{-1}. A plot of the observed first-order rate constant for the growth of this transient *vs* diethylamine concentration yielded a second-order rate constant of 4.5×10^8 M^{-1} s^{-1}, in excellent agreement with that obtained for the decay of phenyl ketene, indicating that this species is the initial product of the reaction of phenyl ketene with diethylamine. This species was not stable, and its decay was also dependent on the diethylamine concentration. It leads to the formation of a stable species observed at 1640 cm^{-1}, growing in with kinetics identical with that observed for the decay of the 1680-cm^{-1} band. Figure 6 shows the TRIR spectrum and kinetic traces observed in this region for the LFP of a solution of α-diazoacetophenone containing 2.5 mM diethylamine. At this concentration of diethylamine, growth of the 1680-cm^{-1} band is instantaneous on the applied time scale, while the decay of this band and the growth of the stable product at 1640 cm^{-1} are clearly concomitant. Plots of the observed first-order decay or growth rate constants *vs* diethylamine concentration yielded values for the second-order rate constants of 2.1×10^7 M^{-1} s^{-1} for the decay of the 1680-cm^{-1} band and 2.0×10^7 M^{-1} s^{-1} for the growth of the stable 1640-cm^{-1} band.

The stable product at 1640 cm^{-1} can be readily identified as *N*,*N*-diethylphenylacetamide. The assignment of the 1680-cm^{-1} band is more difficult since at least two intermediates can be considered as initial products of the reaction of ketene with amine. Transient species that have been previously observed in a number of ketene reactions with pyridine in solution by time-resolved UV−vis spectroscopy[8,43] were assigned to zwitterionic ylides (Scheme 2) which result from attack of an amine at the C_α position of the ketene. More recently the species identified as such zwitterions were characterized by IR in matrix-isolation studies[15,16] of this reaction with the corresponding bands assigned in the 1650−1730-cm^{-1} region.[44] Similarly, the low-temperature reaction between fluorenylidene ketene and imidazole in a phenolic resin was reported to produce a zwitterionic ylide characterized by an absorption at 1635 cm^{-1} in the IR.[46] Following these leads, in our own recent LFP-TRIR studies of the reaction of fluorenylidene ketene with diethylamine, the band at 1674 cm^{-1} was assigned to the corresponding initial zwitterionic product.[20] In this reaction, however, as in the reaction of phenyl ketene with diethylamine (Scheme 3), it is possible to envisage that the first observable intermediate is an amide enol formed either directly through the four-membered-ring transition state[47] or via a short-lived zwitterionic intermediate, and not the zwitterionic ylide itself. To our knowledge, there has been only one direct observation of amide enol: by ^{1}H NMR in the reaction of bis(2,4,6-triisopropylphenyl)acetic acid with Me_2NH.[48] IR bands corresponding to the C=C stretching frequency of the amide enols should occur in a similar region to that of the corresponding ketene *O*,*N*-acetals.[49] For a family of dimethyl ketene *O*,*N*-acetals, $Me_2C{=}C(OR^1)NR^2R^3$, these frequencies were measured in the 1640−1680 cm^{-1} region of the spectrum.[52] They correspond very well to the bands we observed at 1680 and 1674 cm^{-1}, respectively, for the initial products in the reactions of phenyl ketene and fluorenylidene ketene[20] with diethylamine. Thus, these bands may well correspond to the appropriate amide enols.

Scheme 2

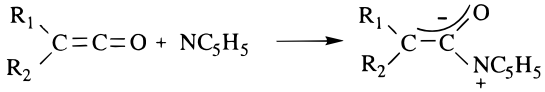

Our current data do not allow for unequivocal identification of the species that are observed in the reaction of phenyl ketene with diethylamine. The existing evidence indicates that the 1680-cm^{-1} band could correspond either to the zwitterion **3** or the amide enol **4**.

Recent theoretical treatment of a prototypical reaction of ketene with ammonia[53] supports the notion of the initial addition

(43) Wang, J.-L.; Toscano, J. P.; Platz, M. S.; Nikolaev, V.; Popic, V. *J. Am. Chem. Soc.* **1995**, *117*, 5477−5483. Boate, D. R.; Johnston, L. J.; Kwong, P. C.; Lee-Ruff, E.; Scaiano, J. C. *J. Am. Chem. Soc.* **1990**, *112*, 8858−8863. Barra, M.; Fisher, T. A.; Cernigliaro, G. J.; Sinta, R.; Scaiano, J. C. *J. Am. Chem. Soc.* **1992**, *114*, 2630−2634.

(44) Recently a relevant zwitterionic complex

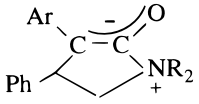

where Ar = $C_6H_5Cr(CO)_3$ and R_2 = $(CH_2)_5$, was isolated and its X-ray structure established, suggesting a similarity of the C=O bond length in the complex and in an amide moiety.[45]

(45) Chelain, E.; Goumont, R.; Hamon, L.; Parlier, A.; Rudler, M.; Rudler, H.; Daran, J.-C.; Vaissermann, J. *J. Am. Chem. Soc.* **1992**, *114*, 8088−8098.

(46) Pacansky, J.; Chang, J. S.; Brown, D. W.; Schwarz, W. *J. Org. Chem.* **1982**, *47*, 2233−2234.

(47) Such a transition state may be extended by inclusion of the solvent molecule(s).

(48) Frey, J.; Rappoport, Z. *J. Am. Chem. Soc.* **1996**, *118*, 3994−3995.

(49) For related systems, the C=C stretch was observed at 1661.9 cm^{-1} in matrix-isolation studies of *syn*-vinyl alcohol[50] and in the range of 1610−1680 cm^{-1} for a family of vinyl ethers.[51]

(50) Rodler, M.; Blom, C. E.; Bauder, A. *J. Am. Chem. Soc.* **1984**, *106*, 4029−4035.

(51) *The Aldrich Library of FT-IR Spectra*, 1st ed.; Pouchert, C. J., Ed.; Aldrich: New York, 1985; Vol. I.

(52) Schaumann, E.; Sieveking, S.; Walter, W. *Chem. Ber.* **1974**, *107*, 3589−3601.

(53) Tidwell, T. T.; Sung, S. *J. Am. Chem. Soc.*, in press.

Scheme 3

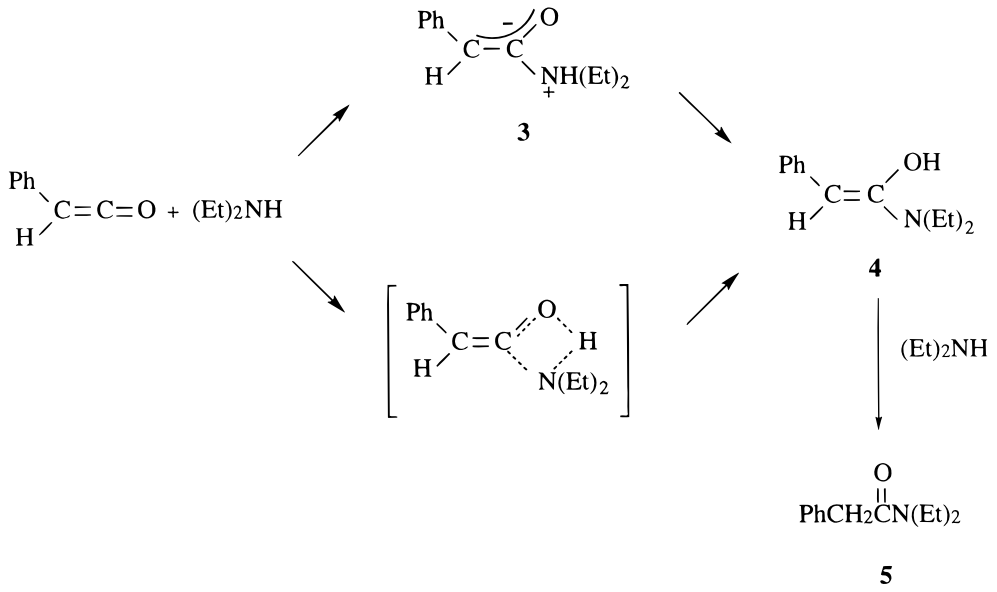

Table 2. Bimolecular Rate Constants for the Reaction of Ketenes with Amines in Acetonitrile Solution at 23 °C (Estimated Error ±20%)

	ketene		$k_q/10^7$ M^{-1} s^{-1}						
no.	R_1	R_2	N [a]	Et_3N[a]	Et_2NH[b]	NH [b]	*i*-$PrNH_2$[b]	*n*-$BuNH_2$[b]	$PhCH_2NH_2$[b]
Ia	H	*t*-Bu	<0.01	<0.01	0.046	0.67	0.077	0.16	0.075
IIa	H	Ph	<0.01	0.023	48	50	12	33	14
IIIa	H	*p*-MeOPh	<0.01	0.028	33	51	9.5	22	9.2
IVa	H	*p*-CNPh	*c*	*c*	95	140	58	87	58
Va	H	*p*-NO_2Ph	*c*	*c*	95	160	81	110	70
VIa	H	PhC≡C	nm[d]	nm[d]	110	nm[d]	nm[d]	nm[d]	nm[d]
VIIa	H	PhCH═CH	<0.01	0.011	49	80	16	51	17
IXa	Ph	Ph	<0.01	<0.01	1.2	1.5	0.44	1.1	0.54
Xa	Ph	O ‖ PhC	<0.01	<0.01	2.1	3.8	0.94	2.3	1.1

[a] Amine concentrations in the range of 0.14−1.0 M were used for the quenching experiments. [b] Amine concentrations in the range of 0.05−1.2 M were used for the quenching experiments with Ia, 0.05−3.0 mM with IIa−VIa, and 1−30 mM with IXa and Xa. [c] Decays were not first-order. [d] Not measured.

to the carbonyl bond of the ketene with the barrier for this process being smaller by 9−13 kcal/mol than that for the addition to the C═C bond. Theory also predicts[53] that the activation energy for the addition process is much lower for the ammonia dimer compared with that calculated for a monomer. Our observation of the linear dependence of the rate constant for the addition on an amine indicates that in solution, within the concentration range studied, the transition state for the monomeric amine addition is solvent stabilized and the reaction does not require co-association of another molecule of amine to proceed. Theory also predicts[53] a much higher stability (by ca. 30 kcal/mol) of the amide compared with the amide enol. If the 1680-cm^{-1} band observed in the reaction of phenyl ketene with diethylamine corresponds to the amide enol **4**, our experimental data on its conversion to amide **5** corroborate nicely with this calculation. The observed linear dependence of the rate constant of the conversion with diethylamine concentration indicates that this step is base-catalyzed.

A compilation of the kinetic data obtained in this study for ketene quenching by amines is given in Table 2. Our data show a general trend, indicating a much higher reactivity (*ca*. 3 orders of magnitude difference in the corresponding rate constants) of secondary amines compared with that of tertiary amines. Secondary diethylamine shows reactivity similar to those observed for primary amines, while secondary piperidine seems to be in general somewhat more reactive. Recent detailed studies of the kinetics of amine addition reactions to diphenyl ketene in aqueous solutions showed a very similar reactivity pattern.[7] For example, for structurally relevant amines, the values of 3.52×10^5 M^{-1} s^{-1} for *n*-butylamine, 1.94×10^5 M^{-1} s^{-1} for methylamine, 1.03×10^5 M^{-1} s^{-1} for piperidine, 1.91×10^5 M^{-1} s^{-1} for pyrrolidine, and 4.01×10^2 M^{-1} s^{-1} for *N*-methylpiperidine were reported.[7] These rate constants are ca. 2 orders of magnitude lower than those observed in our studies. The decrease in reactivity of amine nucleophiles in aqueous solutions has been reported before, for example, in the reaction of amines with diarylmethyl cations.[54] The second-order rate constant for quenching by *n*-propylamine was found to be 2 orders of magnitude lower in water than in acetonitrile.[54] This was explained by a reaction mechanism in which the hydrated amine complex, $RNH_2\cdots HOH$, is unreactive and, hence, an equilibrium desolvation must precede the quenching reaction.

The observed trend of reactivities suggests[7] that amine addition to ketenes proceeds through direct nucleophilic attack and that the basic strength of the amines that in general follows the order of tertiary > secondary > primary is not a dominant factor controlling the reactivity. Other considerations such as

(54) McClelland, R. A.; Kanagasabapathy, V. M.; Banait, N. S.; Steenken, S. *J. Am. Chem. Soc.* **1992**, *114*, 1816−1823.

steric hindrance have to be taken into account. The nucleophilic attack occurs on the LUMO in the ketene plane.[1] Thus, ketene substituents, which also lie in the plane, could significantly hinder a nucleophile approach as would bulky groups on the attacking amine. Such steric effects are likely contributing to the much lower reactivity of diphenyl ketene compared with monosubstituted ketenes. They are also likely dominant in lowering the reactivity of the tertiary amines. A small decrease of the reactivities of isopropyl- and benzylamines compared to *n*-butylamine as well as a gentle increase of the reactivity of piperidine compared with diethylamine can possibly be attributed to steric effects. Nucleophilic addition to ketenes is likely to proceed via a highly polar transition state. The ability of the system to stabilize developing charges would be important in determining the energetics and kinetics of the reaction. Such a property of the phenyl group is most likely responsible for the much greater reactivity of phenyl ketene compared with that of *tert*-butyl ketene. Although limited, our data on para-substituted phenyl ketenes provide support for the negative charge development on the ketene moiety in the transition state, with electron-withdrawing substituents accelerating and electron-releasing substituents slowing down the process. Hammett treatment with the σ_p parameters yields ρ values of 0.43 (correlation coefficient, cc = 0.994), 0.50 (cc = 0.973), 0.88 (cc = 0.991), 0.63 (cc = 0.999), and 0.83 (cc = 0.999) for diethylamine, piperidine, and isopropyl-, *n*-butyl-, and benzylamines, respectively. It is worth noting that similar treatment of the kinetic data for the hydration of para-substituted phenyl ketenes in aqueous solution yielded a ρ value of 1.19,[55] indicating a possibly higher polarity of the transition state for hydration than that for amine attack. With our set of data on amine additions and those known for the hydration reactions,[56] it is possible to correlate the trends of reactivities for these two processes for the entire group of ketenes included in our studies. Across the group, for all ketenes, the rectivities with amine and water seem to follow the same general trend, although a larger spread of the relative rate constants is observed for the hydration reaction. The latter may reflect the higher polarity of the aqueous medium and/or the transition state of the reaction.

Experimental Section

Materials. Acetonitrile (BDH Omnisolve), piperidine (BDH), diethylamine (BDH), isopropylamine (Aldrich), *n*-butylamine (Aldrich), benzylamine (Aldrich), 2*H*-pyran-2-one (VIII, Aldrich), triethylamine (Fisher), and pyridine (Anachemia) were used as received. Precursors I,[9] II,[6,57] IV,[3,57] VII,[10,57] IX,[6] and X[58] were kindly supplied by Prof. A. J. Kresge and used without further purification. Precursor VI[10] was kindly supplied by Prof. T. T. Tidwell and used without further purification. Precursor V[59] was kindly supplied by Prof. M. H. Liu and used without further purification.

α-Diazo-*p*-methoxyacetophenone (III). To a stirred suspension of sodium hydroxide (1.0 g, 41.7 mmol) in anhydrous ether (100 mL) was added *p*-methoxyacetophenone (5.0 g, 33.3 mmol) and an excess of ethyl formate (12.0 g, 162 mmol). After GC−MS analysis revealed complete consumption of the *p*-methoxyacetophenone (*ca*. 2 h), ethanol (5 mL) was added, followed by 0.1 N aqueous HCl (100 mL). The solution was extracted with diethyl ether and dried over magnesium sulfate. Removal of the solvent yielded a solid, which was recrystallized 3 times from hexane (mp 54−56 °C). This was identified by GC−MS as α-formyl-*p*-methoxyacetophenone (yield 56%). A solution of sodium ethoxide was prepared by adding sodium metal (0.15 g, 6.52 mmol) to ethanol (20 mL) in a round-bottom flask fitted with a reflux condenser. To this solution, α-formyl-*p*-methoxyacetophenone (1.0 g, 5.62 mmol) was added, and the solution was stirred for 30 min, resulting in the precipitation of a white solid. Mesyl azide[60] (0.75 g, 6.2 mmol) was then added and the mixture stirred at room temperature in the dark for 2 h. The completion of the reaction was noted by complete dissolution of the precipitate and the formation of a deep red solution. To the reaction mixture was added 10% aqueous NaOH (50 mL), followed by extraction with diethyl ether (3 × 20 mL). The combined ethereal extracts were dried, and the ether was removed, yielding a brown oil. This was dissolved in a mixture of hexane and diethyl ether to yield a yellow solution, which was filtered and rotary evaporated. The resulting solid was recrystallized 3 times from 50/50 benzene/hexane, yielding yellow crystalline plates (yield 20%). HRMS Calcd: 176.1128. Found: 176.0501. Mp: 85−86 °C. IR (CH_3CN solution): 2108 (CN_2), 1616 cm^{-1} (C═O). ^1H NMR ($CDCl_3$): δ (ppm) 3.86 (s, 3 H, O*CH*$_3$), 5.85 (s, 1 H, N_2CH), 6.93 (d, 2 H, aromatic), 7.74 (d, 2 H, aromatic). ^{13}C NMR ($CDCl_3$): 185.38, 163.48, 129.72, 114.01, 55.68, 53.68.

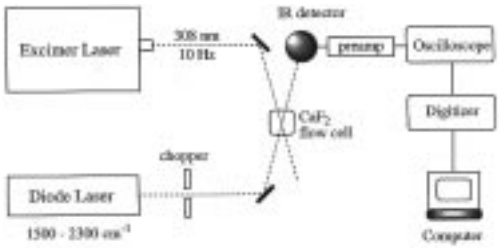

Figure 7. Schematic diagram of the laser flash photolysis system with time-resolved infrared detection (LFP-TRIR).

Time-Resolved Infrared (TRIR) Measurements. Figure 7 shows a schematic diagram of the TRIR system. Previously, only details of a much earlier version of the system[61,62] or brief descriptions of the current system[18] have been given; full details of the current system are therefore presented herein. Solutions (prepared to give an absorbance of 0.3 at 308 nm) were flowed through a CaF_2 cell, the path length of which was adjustable from 0.5 to 6 mm. The output of a Lumonics Excimer-500 laser (XeCl, 308 nm; 10-ns pulse width; 10-Hz repetition rate) was focused onto the sample cell from one side. The absorption by the solution of these excitation pulses generated the transients of interest. The output of a Mutek Model MPS-1000 diode laser was passed through the solution cell from the opposite side as the excitation pulses and focused onto a CdHgTe semiconductor IR detector, mounted on a liquid N_2 Dewar. This detector output a voltage directly proportional to the incident IR intensity and had a response time of *ca*. 250 ns. The diode laser contained ports for four different diodes, the temperature of which were controlled in the range of 20−90 K by a liquid He cryostat. By varying the temperature of and current passing through the diode, a tuning range of approximately 200 cm^{-1} was obtained for each diode, yielding a total range of the system of 800 cm^{-1}. The diodes currently installed gave a nearly continuous tuning range from 1500 to 2300 cm^{-1}. The spectral width of the diode laser output was less than 1 cm^{-1}. The temperature and current were set manually; the frequency of the resulting output was determined using a Mutek Model MDS-1200 monochromator. The cw diode laser output was chopped to give a square-wave IR probe of 10-Hz frequency and 500-ms duration. This was necessary both to provide the timing trigger for the excimer laser and the electronics and to prevent saturation of

(55) Bothe, E.; Meier, H.; Schulte-Frohlinde, D.; von Sonntag, C. *Angew. Chem., Int. Ed. Engl*. **1976**, *15*, 380−381.

(56) The corresponding rate constants in water are for Ia, 14.6 s^{-1}; for IIa, 4.77 × 10^3 s^{-1}; for IIIa, 4.5 × 10^3 s^{-1}; for IVa, 25.6 × 10^3 s^{-1}; for Va, 49.5 × 10^3 s^{-1}; for VIa, 71.6 × 10^3 s^{-1}; for VIIa, 5.76 × 10^3 s^{-1}; for IXa, 0.275 × 10^3 s^{-1}; and for Xa, 6.29 × 10^3 s^{-1}. See ref 1b, pp 578−580.

(57) Danheiser, R. L.; Miller, R. F.; Brisbois, R. G.; Park, S. Z. *J. Org. Chem.* **1990**, *55*, 1959−1964.

(58) Popic, V. V.; Korneev, S. M.; Nikolaev, V. A.; Korobitsyna, I. K. *Synthesis* **1991**, 195−198.

(59) Bradley, W.; Schwarzenbach, G. *J. Chem. Soc*. **1928**, 2904−2912.

(60) Boyer, J. H.; Mack, C. H.; Goebel, W.; Morgan, L. R., Jr. *J. Org. Chem.* **1958**, *23*, 1051−1053. Taber, D. F.; Ruckle, R. E., Jr.; Hennessy, M. J. *J. Org. Chem.* **1986**, *51*, 4077−4078.

(61) Rayner, D. M.; Nazran, A. S.; Drouin, M.; Hackett, P. A. *J. Phys. Chem.* **1986**, *90*, 2882−2888.

(62) Ishikawa, Y.; Hackett, P. A.; Rayner, D. M. *J. Phys. Chem*. **1988**, *92*, 3863−3869.

the IR detector. The synchronous relative timing of the excimer laser and electronics was controlled using the chopper signal by a Stanford Model DG535 delay generator.

The kinetic traces at a particular IR frequency were obtained by measuring the IR intensity (as a voltage at the detector) passing through the sample before, during, and after absorption of the UV laser pulse. The detector signal was observed on a Tektronix Model 7603 oscilloscope as voltage *vs* time. This oscilloscope trace was then digitized using a DSP Technology Model 6001 transient digitizer, controlled by a OGIVAR 386 computer. Absorption of the excitation pulse sometimes caused a shock wave in the kinetic traces, which is dependent on the solution and path length. In such cases, all kinetic traces were corrected after data acquisition by subtracting the shock wave measured at an IR frequency at which no transient was observed. If no shock wave was observed, then the kinetic traces were corrected by subtracting the trace measured with the excimer beam blocked from hitting the sample. This is preferable, as the detector signal was not flat, due to detector saturation, and the slope of this signal was dependent on the signal strength. Spectra were obtained by measuring the individual kinetic traces at 2−10-cm^{-1} increments throughout the region of interest and plotting Δ absorbance *vs* wavenumber for a fixed time after the UV pulse.

Acknowledgment. We are grateful to Prof. T. T. Tidwell for valuable discussions and sharing the results prior to publication and to Prof. A. J. Kresge for valuable comments.

JA964155B